Cement & Concrete Composites 32 (2010) 708–717

Contents lists available at ScienceDirect

Cement & Concrete Composites

journal homepage: www.elsevier.com/locate/cemconcomp

Hardened properties of self-consolidating high performance concrete including rice husk ash

Md. Safiuddin *, J.S. West, K.A. Soudki

Department of Civil and Environmental Engineering, Faculty of Engineering, University of Waterloo, Waterloo, Ontario, Canada N2L 3G1

ARTICLE INFO

Article history:
Received 21 October 2008
Received in revised form 25 May 2010
Accepted 9 July 2010
Available online 14 July 2010

Keywords:
Air content
Concrete
Hardened properties
Rice husk ash
Water/binder ratio

ABSTRACT

This paper mainly presents the key hardened properties of self-consolidating high performance concrete (SCHPC). Various SCHPCs were produced with different water/binder (W/B) ratios, rice husk ash (RHA) contents, and air contents. The required filling ability and air content were achieved in all freshly mixed SCHPCs. The hardened SCHPCs were tested for compressive strength, ultrasonic pulse velocity, water absorption, total porosity, and true electrical resistivity. The effects of W/B ratio, RHA content, and air content on these hardened properties were observed. Test results revealed that the compressive strength, ultrasonic pulse velocity, and electrical resistivity increased whereas the water absorption and total porosity decreased with lower W/B ratio and higher RHA content. In addition, the air content decreased the compressive strength, ultrasonic pulse velocity, water absorption, and total porosity but increased the electrical resistivity. Based on the overall effects of rice husk ash, the optimum RHA content for SCHPC has been defined.

1. Introduction

Advancements in concrete technology have resulted in the development of a new type of concrete, which is known as self-consolidating high performance concrete (SCHPC). The merits of SCHPC are based on the concept of self-consolidating and high performance concretes. Self-consolidating concrete (SCC) is a highly flowing concrete that spreads through congested reinforcement, reaches every corner of the formwork, and is consolidated under its own weight without vibration or any other means of consolidation [1]. SCC must require excellent filling ability, good passing ability, and adequate segregation resistance. However, it does not include high strength and good durability as the essential performance criteria. Conversely, high performance concrete (HPC) has been defined as a concrete that is properly designed, mixed, placed, consolidated, and cured to provide high strength and low transport properties or good durability [2]. HPC generally exhibits a good segregation resistance. But it does not provide excellent filling ability and good passing ability like SCC, and therefore needs an external means such as rodding or vibration for proper consolidation. When the performance criteria for high strength and low transport properties or good durability of HPC are included in SCC with a lower water/binder (W/B) ratio, it can be referred to as SCHPC. Hence, an SCHPC is a special concrete, which offers excellent filling ability and passing ability, adequate segregation resistance, high strength, and low transport properties or good durability. The performance criteria, which should be satisfied for the major fresh and hardened properties of SCHPC are given in Table 1.

SCHPC is produced by exploiting the benefits of high-range water reducer (HRWR) and supplementary cementing material (SCM). The use of HRWR is essential to produce SCHPC. A HRWR contributes to achieve excellent filling ability and passing ability in fresh SCHPC. The hardened properties of SCHPC are also improved in the presence of HRWR due to the enhanced dispersion of binder particles and improved paste densification. Along with HRWR, SCMs are generally incorporated in SCHPC to enhance the strength and durability, and to reduce the cement content of concrete. Several well-known SCMs such as silica fume, ground granulated blast-furnace slag, and fly ash have been used to produce SCHPC [9,15–17]. However, the expense of several common SCMs such as silica fume and high reactivity metakaolin increases the overall material cost of SCHPC. In particular, the use of silica fume may be cost-prohibitive in developing countries. Therefore, it is necessary to use an alternative less expensive SCM such as rice husk ash (RHA) to produce cost-effective SCHPC.

RHA is typically obtained by the controlled burning of rice husks at 500–800 °C (conventional thermal treatment) [18]. The quality of RHA can be improved by pre-treating the rice husks with an acid leaching and then burning them under controlled conditions (chemical–thermal treatment) [19]. If processed and used properly, RHA offers similar benefits like silica fume with regard to the improved hardened properties and durability of concrete

* Corresponding author. Tel.: +1 519 888 4567x32344; fax: +1 519 888 4349.
E-mail addresses: safiq@yahoo.com, msafiudd@engmail.uwaterloo.ca (Md. Safiuddin).

0958-9465/$ - see front matter © 2010 Elsevier Ltd. All rights reserved.
doi:10.1016/j.cemconcomp.2010.07.006

Table 1
Performance criteria for the key fresh and hardened properties of SCHPC.

Test method	Property	Criterion
SCC property		
Slump flow (SF)	Filling ability (flow spread)	550–850 mm [3]
V-funnel flow	Filling ability (flow time)	6–12 s [4]
Orimet flow	Filling ability (flow time)	2.5–9 s [5]
Fill-box flow	Passing ability (filling percentage)	90–100% [4]
L-box flow	Passing ability (blocking ratio)	0.8–1.0 [4]
U-box flow	Passing ability (filling height)	⩽30 mm [4]
J-ring flow (JF)	Passing ability (blocking)	(SF–JF)⩽50 mm [6]
Penetration depth	Segregation resistance	⩽8 mm [7]
Sieve segregation	Segregation resistance	⩽18% [8]
HPC property		
Air content by pressure method	Fresh air content	4–8% [9]
Compression using cylinders	Early-age compressive strengths	>20 MPa [10]
	28 and 91 days compressive strengths	>40 MPa [10]
Ultrasonic pulse velocity by a PUNDIT[a]	Physical quality or condition	⩾4575 m/s [11]
Porosity by fluid displacement method	Total porosity as an indicator of strength and durability	7–15% [12]
Absorption by water saturation technique	Water absorption as an indicator of durability	3–6% [13]
True electrical resistivity by Wenner probe	Electrical resistance to corrosion	>(5–10) kΩ cm [14]
Rapid chloride ion penetration	Electrical charged passed as an indicator of corrosion resistance	<2000 C [10]
Normal chloride ion penetration at 6 months	Penetrated chloride value as an indicator of corrosion resistance	<0.07% [10]
Resistance to freezing and thawing	Durability factor after 300 cycles of freeze–thaw	>0.80 [2]

[a] Portable ultrasonic non-destructive digital indicating tester.

[19–23]. In addition, the usage of RHA minimizes the environmental burden associated with the waste disposal problem caused by the rice milling industry. The recent yearly production of rice in the world is approximately 560 million metric tons [24]. Rice husk constitutes about one fifth of the dried rice [25]. Therefore, nearly 112 million metric tons of rice husks are generated every year. This is causing a large environmental load, which can be reduced if RHA is used in concrete production. Moreover, the use of RHA decreases the demand for cement in the construction industry, and thus reduces the cost of concrete production and lessens the environmental pollution caused by the CO_2 emission from the cement factories. Hence, RHA not only improves the concrete properties and durability, but also provides economic and environmental benefits. Realizing the manifold benefits of RHA, it has been used successfully to produce high strength and high performance concretes [20,21]. Yet, the use of RHA in SCHPC is very limited. No comprehensive research has been conducted to explore the potential of RHA for SCHPC by investigating its effects on the hardened properties and durability of this concrete.

The present study produced a number of SCHPCs utilizing conventional RHA as an SCM. The target slump flow (a measure of filling ability) and air content were maintained in the fresh concretes using adequate dosages of HRWR and air-entraining admixture (AEA), respectively. The effects of RHA were mainly investigated with respect to the key hardened properties of concrete. The effects of W/B ratio and air content on the hardened properties were also observed. Both destructive and non-destructive tests were performed to determine the hardened properties of the concretes. The hardened properties obtained were compressive strength, ultrasonic pulse velocity, water absorption, total porosity, and true electrical resistivity. Based on the effects of rice husk ash observed in the present study, the optimum RHA content for SCHPC was defined.

2. Experimental program

2.1. Constituent materials

Concrete stone, concrete sand, normal portland cement (C), amorphous RHA, normal tap water (W), a polycarboxylate-based HRWR, and a synthetic AEA were used to produce various SCHPCs adopted in the present study.

The concrete stone was a blend of crushed and round aggregates with a maximum size of 19 mm. It was used as the coarse aggregate (CA) for concretes. The weight percentage of round aggregate in concrete stone was 50% of the total aggregate (A). The concrete sand was locally available natural pit sand with a maximum size of 4.75 mm. It was used as the fine aggregate (FA) for concretes. Both concrete stone and sand complied with the grading requirements as mentioned in ASTM C 136. Moreover, the optimum sand/aggregate (S/A) ratio leading to a maximum bulk density in aggregate blend was 0.50. It was obtained by blending different weight proportions of sand and coarse aggregate, and by determining the bulk density of the aggregate blends according to ASTM C 29/C 29M.

Normal portland cement was used as the main cementing material for various SCHPCs. It complied with the physical and chemical requirements of ASTM Type I and CSA Type 10 or Type GU cement. RHA was used as an SCM for different SCHPCs. It was originally collected from North Carolina, USA. RHA was processed from rice husks based on the conventional thermal treatment. It was available in very fine powder form with angular particle size and grey color. The surface fineness of RHA was much higher than that of cement due to the cellular particles with honeycomb microstructure. The Blaine specific surface area of RHA was 2326 m^2/kg and that of cement was 412 m^2/kg. The RHA had an accelerated pozzolanic activity index of 122.4%, which was determined according to the procedure used for silica fume, as given in ASTM C 1240. It was much higher than the required minimum pozzolanic activity indices of fly ash (75%) and silica fume (85%). Moreover, the chemical composition of RHA was obtained based on the borate fusion whole rock analysis by XRF spectrometry. The RHA had a silica content of 93.6%, as observed from its chemical composition. This confirmed the excellent pozzolanicity of RHA as compared with fly ash and silica fume according to the pozzolanic requirements mentioned in ASTM C 618 and ASTM C 1240, respectively. The particle size distribution of RHA was also compared with that of cement. The particle size distribution of cement was determined using the laser diffraction method complied with ISO 13320-1. The hydrometer method as mentioned in ASTM D 422 was used for the particle size analysis of RHA. The results obtained for the par-

ticle size distributions showed that the RHA particles were much finer than cement. The median particle size of RHA was 6 μm whereas that of cement was 15 μm. About 85% of the RHA particles were smaller than 15 μm.

2.2. Mixture proportions

The concrete mixtures were designed based on the W/B ratios of 0.30, 0.35, 0.40 and 0.50, and using RHA substituting 0% to 30% of cement by weight. Cement and RHA acted as the total binder (B) for the concretes. In addition, the optimum S/A ratio of 0.50 leading to a maximum bulk density (minimum void content) in aggregate blend was used for all concrete mixtures. A total air content (AC) of 6% was adopted to design the air-entrained SCHPCs whereas 2% entrapped air content was considered in designing the non-air-entrained SCHPC. The concrete mixtures were designed to obtain a slump flow (SF) in the range of 600–800 mm, which gives an excellent filling ability. The dosages of HRWR were decided to attain the required slump flow. The HRWR dosages used for different SCHPCs were 70–80% of the saturation dosages. The saturation dosages of HRWR were determined by testing the filling ability of the binder paste components of various SCHPCs. The detailed procedure for determining the HRWR saturation dosage has been described in [26]. In addition, the AEA dosages were fixed to achieve a total air content of 6 ± 1.5% in air-entrained SCHPCs. The complete procedure for deciding the AEA dosages has been presented in [27].

The mixture proportions and designations of various SCHPCs are given in Table 2. The concretes were designated based on the W/B ratio, RHA content, and design air content. For example, the 'C30R0A6' designation was used for the concrete prepared with a W/B ratio of 0.30, 0% RHA content, and 6% design air content.

2.3. Preparation of fresh concretes and hardened test specimens

The concrete constituent materials were batched for mixing based on the mixture proportions shown in Table 2. The batch volume of the fresh concretes was taken 15% more than the required to compensate the loss during mixing and testing. The component materials were mixed in a revolving pan-type mixer to produce the fresh SCHPCs. The AEA dosage was added at the beginning whereas the HRWR dosage was used at the later stage of mixing. The net mixing time for all concrete mixtures was 7 min. The detailed mixing procedure for preparing the fresh concretes is depicted in [28].

The hardened test specimens were prepared from the fresh concretes through several steps such as moulding, de-moulding, and curing. In addition, the grinding and cutting operations were performed when necessary. The cylinder specimens of $\varnothing 100 \times 200$ mm size required for testing the compressive strength, ultrasonic pulse velocity, and electrical resistivity of concretes were moulded in single-use plastic moulds. The fresh concrete was poured into the cylinder moulds in one layer, and no vibration or rodding was used for consolidation. Immediately after casting, the cylinder specimens were sealed using plastic lids and left undisturbed at room temperature (23 ± 2 °C). The specimens were de-moulded, marked, and transferred to the fog room for wet curing at the age of 24 ± 4 h. The wet curing was carried out until the day of testing. The curing temperature was 23 ± 2 °C and the relative humidity was above 95%.

The top faces of the moulded $\varnothing 100 \times 200$ mm cylinders were smoothened by grinding to make the ends plane and parallel before testing for the ultrasonic pulse velocity and compressive strength of concrete. This facilitated to achieve a good coupling during the ultrasonic pulse velocity test. It also ensured the perpendicularity of end faces to the axis of specimen during the compression test.

The cylinder specimens of $\varnothing 100 \times 50$ mm size required for determining the water absorption and total porosity of concretes were prepared by cutting a required number of $\varnothing 100 \times 200$ mm moulded and cured cylinders. Thin sections from both ends of the cylinders were discarded to minimize the end effects. Three $\varnothing 100 \times 50$ mm small cylinder specimens were obtained from each $\varnothing 100 \times 200$ mm parent cylinder.

2.4. Test procedures

The fresh SCHPCs were tested to determine the slump flow according to ASTM C 1611/C 1611M with an exception for measuring the diameter of deformed concrete. In the present study, the diameter of the deformed concrete was measured along two pairs (instead of one pair) of diametrical lines that divided the whole flow spread into eight equal segments. The air content of the fresh SCHPCs was determined according to ASTM C 231, except for the consolidation and placement of concrete. The freshly mixed concrete was placed in the air meter in one layer without any consolidation. The fresh SCHPCs were also tested for passing ability, segregation resistance, and other filling ability properties, which

Table 2
Details of the concrete mixture proportions.

Concrete type	Basic proportions (kg/m^3)					Admixture dosages (% B)		SF[a] (mm)	AC[b] (%)
	CA	FA	C	RHA	W	HRWR	AEA		
C30R0A6	846.3	842.2	492.7	0	147.8	0.875	0.026	710	5.7
C30R15A6	829.9	825.8	418.8	73.9	147.8	1.75	0.047	735	5.3
C30R20A6	824.4	820.3	394.2	98.5	147.8	2.10	0.056	770	5.7
C35R0A6	876.1	871.8	422.3	0	147.8	0.70	0.020	690	5.3
C35R5A6	871.4	867.1	401.2	21.1	147.8	0.875	0.025	700	5.5
C35R10A6	866.7	862.4	380.1	42.2	147.8	1.05	0.035	710	5.1
C35R15A6	862.0	857.8	359.0	63.3	147.8	1.40	0.045	720	5.1
C35R20A6	857.3	853.1	337.8	84.5	147.8	1.75	0.054	710	5.0
C35R25A6	852.6	848.4	316.7	105.6	147.8	2.10	0.070	740	5.6
C35R30A6	847.9	843.7	295.6	126.7	147.8	2.45	0.080	750	5.2
C40R0A6	898.4	894.0	369.5	0	147.8	0.60	0.011	665	6.1
C40R15A6	886.0	881.7	314.1	55.4	147.8	1.00	0.040	680	5.2
C40R20A6	881.9	877.6	295.6	73.9	147.8	1.20	0.051	675	5.3
C50R0A6	928.3	923.7	296.8	0	148.4	0.50	0.006	605	5.2
C50R0A2	940.1	935.5	334.8	0	167.4	0.50	0	600	1.8

[a] Slump flow.
[b] Air content.

are beyond the scope of the present paper. The detailed test procedures for these properties are described in [28,29].

The compressive strength, ultrasonic pulse velocity, and true electrical resistivity of the hardened concretes were determined using triplicate ⌀100 × 200 mm cylinders at each testing age. The compression test was carried out at the ages of 3, 7, 28, and 56 days in accordance with ASTM C 39/C 39M.

The ultrasonic pulse velocity of the concretes was determined at the ages of 28 and 56 days according to ASTM C 597. A portable ultrasonic non-destructive digital indicating tester (PUNDIT) was used to determine the transit time of ultrasonic pulse through concrete specimens. The specimens were air-dried at room temperature (23 ± 2 °C) for 24 h prior to the testing of ultrasonic pulse velocity. The drying process helped to obtain a good coupling between the transducers and specimen.

The true electrical resistivity of the concretes was determined at the ages of 28 and 56 days according to the Florida test method FM 5-578 [30]. A portable concrete resistivity meter with a four-point Wenner array probe was used to measure the electrical resistivity. The specimens were always kept saturated during the testing of electrical resistivity to minimize the differential drying effects. The resistivity obtained from the meter was the apparent electrical resistivity of concrete. Hence, a correction factor was applied to obtain the true electrical resistivity. The correction factor was determined based on the procedure described in [31].

The water absorption and total porosity of the concretes were determined at the ages of 28 and 56 days based on the vacuum saturation technique as described in [32]. Triplicate ⌀100 × 50 mm cylinders were vacuum saturated in water and the saturated surface-dry, buoyant, and oven-dry masses of the specimens were measured. The oven-drying was conducted after vacuum saturation to eliminate the effect of microstructural damage due to heating. The water absorption and total porosity were calculated using Eqs. (1) and (2), respectively, and averaged based on the results of three specimens.

$$W_a = \frac{M_s - M_d}{M_d} \times 100\% \quad (1)$$

$$P_t = \frac{M_s - M_d}{M_s - M_b} \times 100\% \quad (2)$$

where: W_a = water absorption (wt.%), P_t = total porosity (vol.%), M_b = buoyant mass of the saturated specimen in water, M_d = oven-dry mass of the specimen in air, M_s = saturated surface-dry mass of the specimen in air.

3. Results and discussion

3.1. Fresh properties

The detailed test results for the fresh properties of various SCHPCs are presented in [28,29]. This paper only highlights the slump flow and air content results in Table 2. The slump flow of the concretes varied in the range of 600–770 mm, which indicates an excellent filling ability of SCHPC [3,4,9]. In addition, the measured air contents of various SCHPCs differed from the design air content by ±1.0%, which is acceptable. The maximum acceptable tolerance for the air content measurement can be in the range of ±1.5% [33].

The filling ability and air content of SCHPC were prone to decrease with lower W/B ratio and higher RHA content mostly due to the increased surface area of total binder. For a given slump flow, the water demand increases with a greater surface area of binder [28]. Therefore, a higher HRWR dosage was needed to achieve the target slump flow of SCHPC, as evident from Table 2. But a greater HRWR dosage impedes the attachment of entrained air-voids onto the binder particles by reducing the attachment sites [34]. In addition, the increased surface area of binder intensifies the viscosity of the paste that tends to collapse some of the air-voids with increased internal pressure [34]. Hence, a greater AEA dosage was also required at lower W/B ratio and higher RHA content to obtain the target air content, as can be seen from Table 2.

3.2. Compressive strength

The average compressive strengths of the concretes are presented in Fig. 1. The gain in compressive strength continued to occur over the 56 days curing period. The 28-days compressive strength varied from 42.7 to 94.1 MPa while the 56-days compressive strength differed from 44.9 to 98.4 MPa for different concretes. The highest level of later-age compressive strength was achieved for C35R30A6, which contained 30% RHA at the W/B ratio of 0.35. Conversely, the lowest level of compressive strength at all

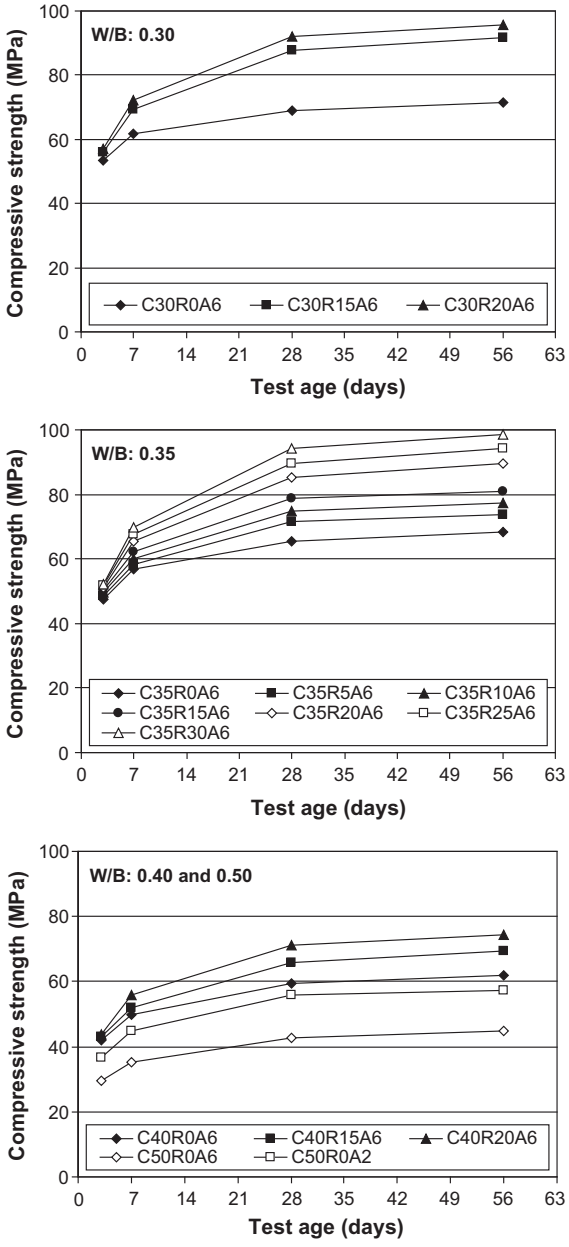

Fig. 1. Compressive strength development of various concretes.

ages was obtained for C50R0A6, which was produced with a W/B ratio of 0.50 and without any RHA. Nevertheless, the performance criteria for both early-age and later-age compressive strengths of SCHPC, as mentioned in Table 1 were fulfilled for all concretes.

The compressive strength of the concretes with and without RHA increased with a lower W/B ratio, as obvious from Fig. 2. The increase in compressive strength is directly related to the reduction in concrete porosity [35]. In the present study, the total porosity of concrete decreased with a lower W/B ratio. The microstructure of concrete is improved in both bulk paste matrix and interfacial transition zone with a reduced porosity [36]. Also, the cement content became higher at a lower W/B ratio since the water content was kept constant for all concretes, as evident from Table 2. The increased cement content improves the physical packing of aggregates and produces a greater amount of calcium silicate hydrate (C–S–H) leading to a higher compressive strength.

The RHA increased the compressive strength of concretes at the ages of 7, 28 and 56 days, as evident from Figs. 1 and 2. The improvement of compressive strength is mostly due to the microfilling ability and pozzolanic activity of RHA [37,38]. With a smaller particle size, the RHA can fill the microvoids within the cement particles. Also, the RHA is a highly reactive SCM. It readily reacts with water and calcium hydroxide (a by-product of cement hydration) and produces additional C–S–H [38]. The additional C–S–H reduces the porosity of concrete by filling the capillary pores, and thus improves the microstructure of concrete in bulk paste matrix and transition zone leading to an increased compressive strength.

The increased air content decreased the compressive strength of concrete. This is obvious from the compressive strength results of the concretes 'C50R0A2' and 'C50R0A6', as presented in Fig. 1. The reduction in compressive strength was about 4 MPa per 1% increase in air content. This is due to the entrained air-voids that increase the total void content of concrete [35]. The increased void content decreases the load carrying capacity of concrete, and thus produces a lower compressive strength.

3.3. Ultrasonic pulse velocity

The average test results for the 28 and 56 days ultrasonic pulse velocity of the concretes are presented in Fig. 3. The ultrasonic pulse velocity varied in the range of 4.730–5.097 km/s, thus indicating an excellent physical condition of the concretes. This is because an ultrasonic pulse velocity higher than 4.575 km/s generally represents the excellent quality of concrete [11]. The excellent

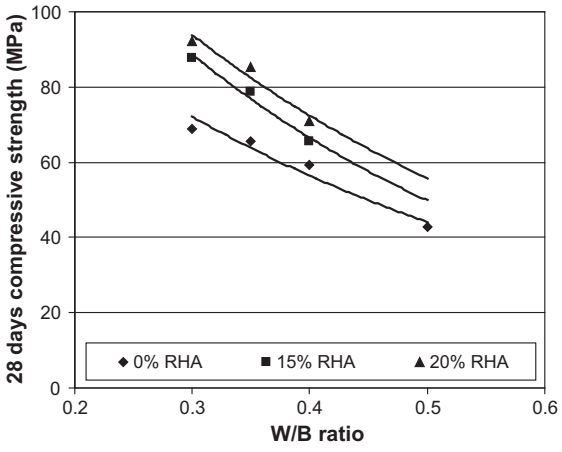

Fig. 2. Effects of W/B ratio and RHA content on the compressive strength of concrete.

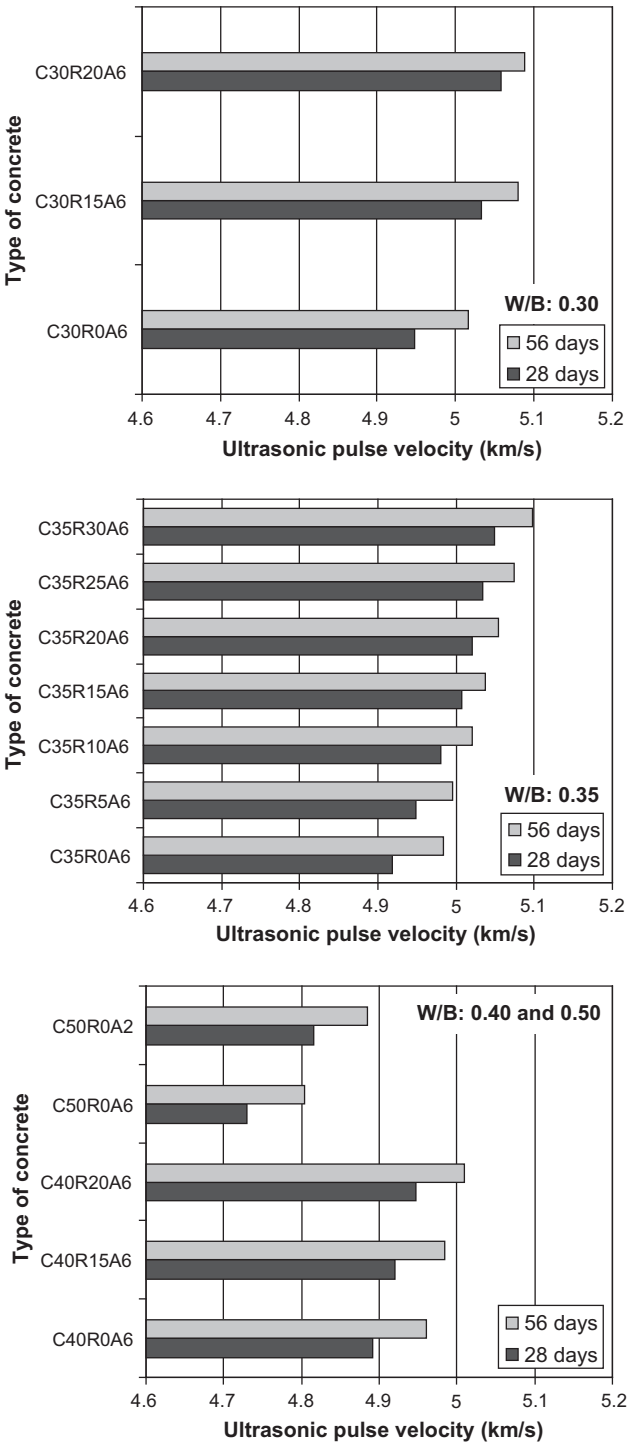

Fig. 3. Ultrasonic pulse velocity of various concretes.

ultrasonic pulse velocity was attained mostly due to the improved pore structure of concretes with reduced porosity and small pore sizes.

The ultrasonic pulse velocity of the concretes with and without RHA increased with a lower W/B ratio, as evident from Fig. 4. The highest level of ultrasonic pulse velocity was achieved for the concretes prepared with the W/B ratio of 0.30. In contrast, the lowest level of ultrasonic pulse velocity was obtained for the concretes produced with the W/B ratio of 0.50. The improvement in ultrasonic pulse velocity at a lower W/B ratio was due to the reduced

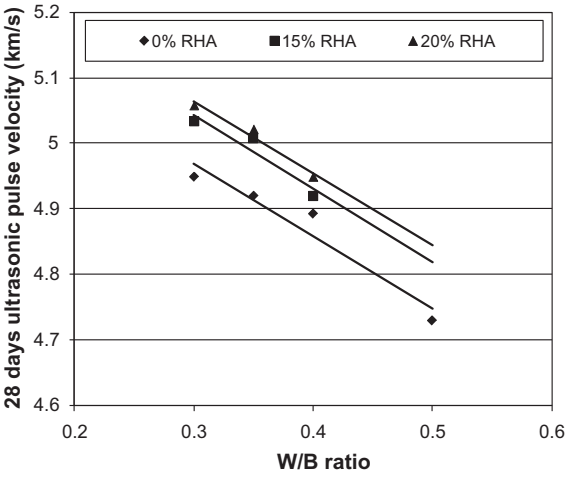

Fig. 4. Effects of W/B ratio and RHA content on the ultrasonic pulse velocity of concrete.

porosity of concrete resulting from a greater volume of hydration products.

The presence of RHA increased the ultrasonic pulse velocity of the concretes, as can be seen from Figs. 3 and 4. The physical and chemical modifications of the pore structure of concrete occur in the presence of RHA due to its microfilling and pozzolanic effects as discussed in Section 3.2. This results in the pore refinement and porosity reduction leading to a dense pore structure in both bulk paste matrix and transition zone of concrete that contributes to a higher ultrasonic pulse velocity. However, the increase in ultrasonic pulse velocity was not as significant as the increase in compressive strength due to the reduced aggregate content. The aggregate content decreased with the increase in RHA content, as can be seen from Table 2. This can diminish the positive effect of RHA on the ultrasonic pulse velocity of concrete, since a reduction in aggregate content decreases the ultrasonic pulse velocity of concrete [11,39].

The ultrasonic pulse velocity of concrete was affected by the entrained air-voids of concrete. It can be seen from Fig. 3 that the ultrasonic pulse velocity of the non-air-entrained concrete (C50R0A2) was higher than that of air-entrained concrete (C50R0A6) produced with the same W/B ratio. This is due to the greater number of pores and C–S–H gel/pore interfaces in the presence of entrained air-voids that may delay the propagation of the ultrasonic pulse, thus reducing its velocity through concrete.

3.4. Water absorption

The average test results for the water absorption of the concretes at 28 and 56 days are illustrated in Fig. 5. The water absorption varied in the range of 2.89–5.97%, which is relatively low. This is consistent with the acceptable range of water absorption for SCHPC, as mentioned in Table 1. The water absorption of high-quality concrete is usually less than 5% [10]. The low range of water absorption was obtained due to the limited pore connectivity and reduced porosity of the concretes.

The water absorption of the concretes with and without RHA decreased with a lower W/B ratio, as obvious from Fig. 6. The highest level of water absorption was obtained for the concretes prepared with the W/B ratio of 0.50. Conversely, the lowest level of water absorption was achieved for the concrete produced with the W/B ratio of 0.30. The decrease in water absorption at the W/B ratio of 0.30 was about 25% in comparison with the W/B ratio

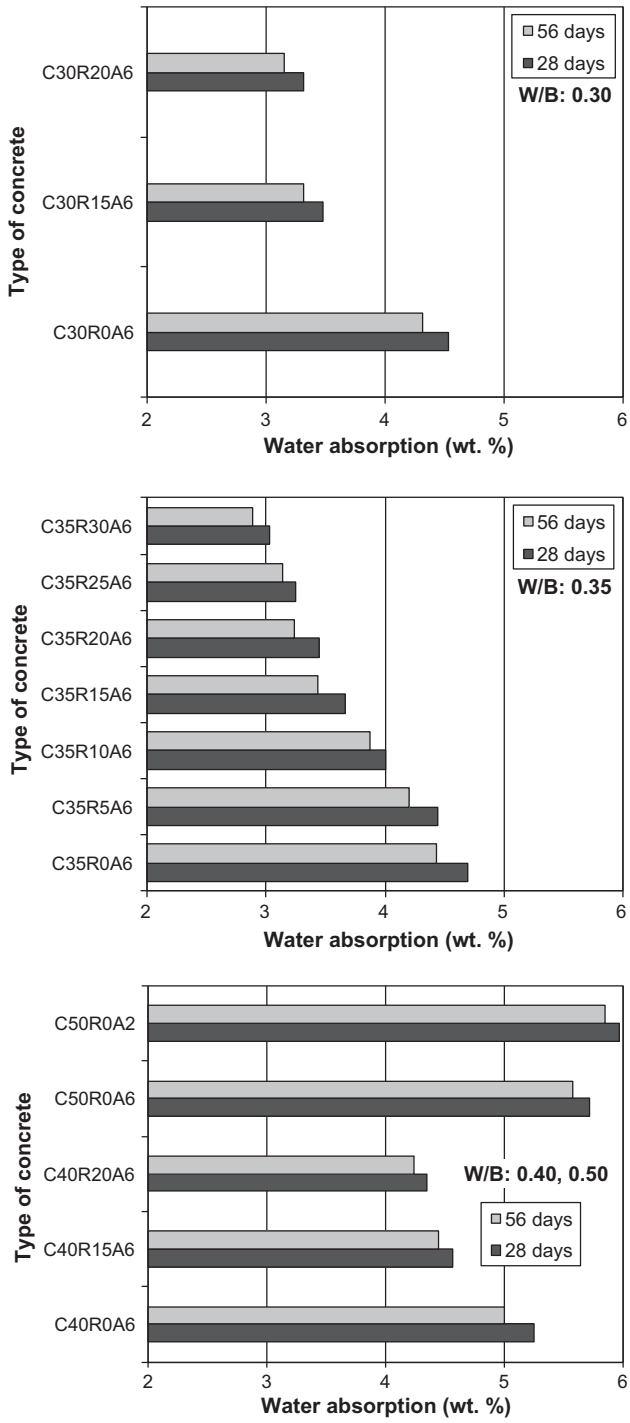

Fig. 5. Water absorption of various concretes.

of 0.50. The significant reduction in the water absorption at a lower W/B ratio is mainly due to the reasons as discussed in Section 3.2.

The water absorption of the concretes decreased with a greater RHA content, as evident from Figs. 5 and 6. The lowest level of water absorption was attained for 30% RHA used in the concrete 'C35R30A6', which provided about 35% reduced water absorption than C35R0A6 at 28 and 56 days. This significant reduction in water absorption is primarily credited to the reduced porosity at a higher RHA content.

The water absorption of concrete was slightly reduced in the presence of entrained air-voids. It can be seen from Fig. 5 that

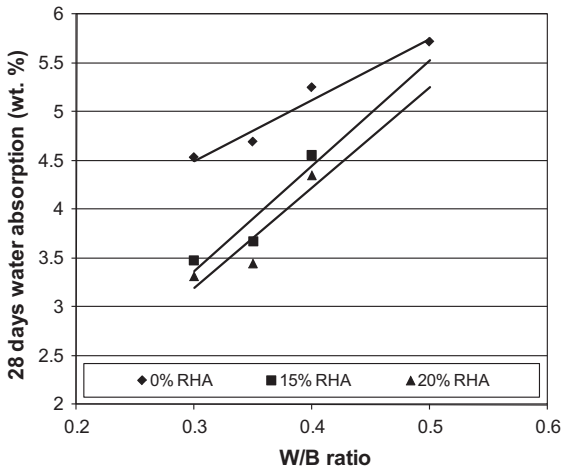

Fig. 6. Effects of W/B ratio and RHA content on the water absorption of concrete.

the concrete 'C50R0A6' containing 5.2% total air content provided a lower water absorption than the concrete 'C50R0A2' with 1.8% entrapped air content. The reason is that the total porosity and pore connectivity of C50R0A6 were reduced due to the presence of unconnected entrained air-voids.

3.5. Total porosity

The average test results for the 28 and 56 days total porosity of the concretes are illustrated in Fig. 7. The total porosity varied in the range of 6.77–13.71%. This is consistent with the acceptable range of total porosity for SCHPC as mentioned in Table 1. The overall test results of total porosity suggest that the quality of the concretes was good. The total porosity of high-quality concrete is about 7% whereas that of average-quality concrete is 15% [12]. The lowest level of total porosity was obtained due to the use of optimum S/A ratio and HRWR. The packing of aggregates is improved and the void content becomes minimal at the optimum S/A ratio. In addition, the HRWR induces a high consistency in concrete, and thus improves the packing in the range of the fines. Also, the HRWR enhances the hydration process by dispersing the cement grains. Thus, both total porosity and pore size are reduced in concretes.

The total porosity of the concretes with and without RHA increased with a higher W/B ratio, as obvious from Fig. 8. The reasons for this behaviour are similar as discussed in Sections 3.2 and 3.3. Furthermore, the total porosity of the concretes was relatively high at the W/B ratio of 0.50. It is possibly due to the fact that this W/B ratio was higher than the minimum W/B ratio needed to eliminate the capillary pores. For a W/B ratio greater than 0.38, the bulk volume of C–S–H gel is not sufficient to fill all water-filled pores and therefore some capillary pores still can remain in the binder paste even after complete hydration [12,35]. Thus, the total porosity of concrete appears to be higher at the W/B ratio of 0.50.

The total porosity of the concretes decreased with greater RHA content, as can be seen from Figs. 7 and 8. The reduction in the total porosity of concrete was 5–35% for various RHA contents. Thus, it was understood that the physical (microfilling) and chemical (pozzolanic) effects of RHA modified the open channels at the cement paste matrix and transition zone of concrete leading to a discontinuous pore structure with reduced porosity.

The total porosity was influenced by the air content of concrete. The air-entrained concrete 'C50R0A6' provided a lower total porosity than the non-air-entrained concrete 'C50R0A2', as obvious from Fig. 7. This is due to the combined effects of reduced water content

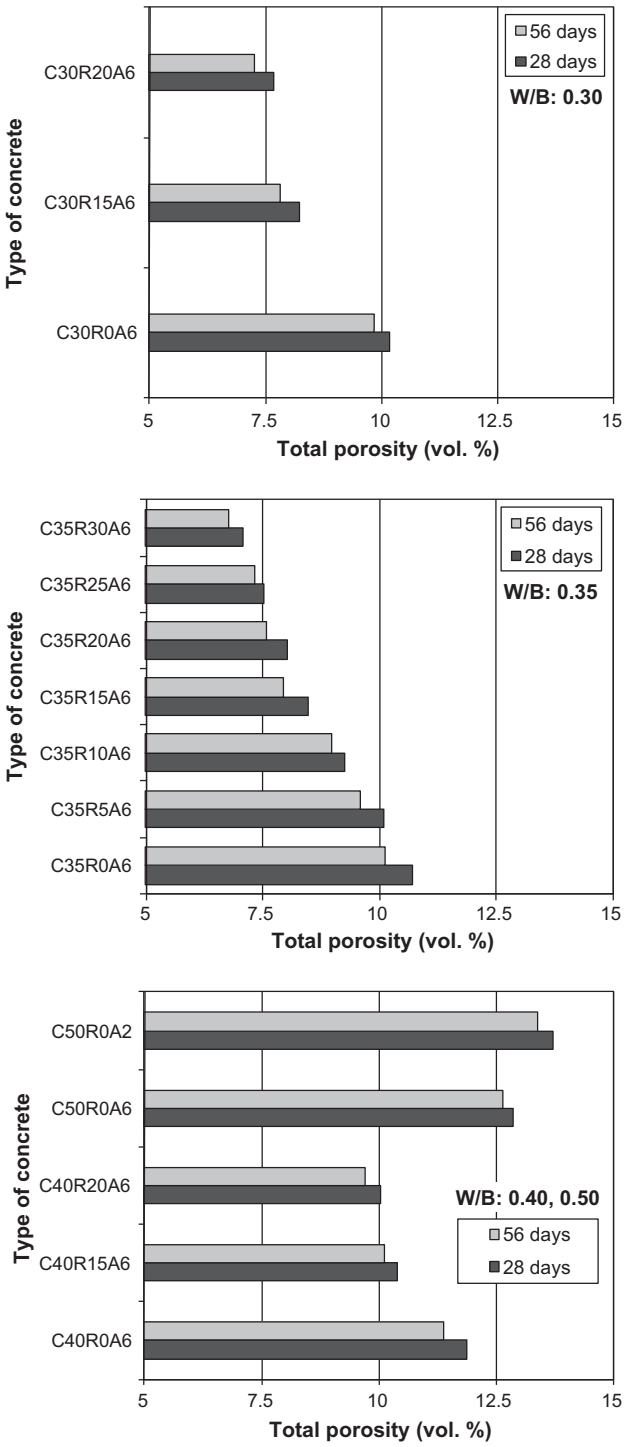

Fig. 7. Total porosity of various concretes.

and non-connectivity of the entrained air-voids. Also, the total volume of capillary pores becomes lower in air-entrained concrete since a part of the gross volume of hardened cement paste is occupied by the unconnected entrained air-voids [35].

3.6. True electrical resistivity

The average test results for the true electrical resistivity of the concretes at 28 and 56 days are presented in Fig. 9. The true electrical resistivity varied in the range of 4.1–121.2 kΩ cm for different types of concrete. The concrete exhibits moderate to low

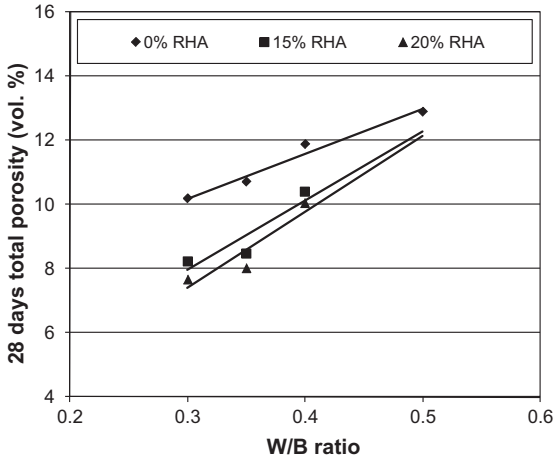

Fig. 8. Effects of W/B ratio and RHA content on the total porosity of concrete.

corrosion rate when its true electrical resistivity is between 5 and 10 kΩ cm (refer to Table 1), whereas good corrosion resistance is obtained when the true electrical resistivity is above 10 kΩ cm [14,35]. All RHA concretes provided a true electrical resistivity higher than 10 kΩ cm. In contrast, the non-RHA concretes exhibited a true electrical resistivity in the range of 4.1–8.9 kΩ cm.

The true electrical resistivity of the concretes with and without RHA increased with a lower W/B ratio, as obvious from Fig. 10. The highest level of true electrical resistivity was observed at the W/B ratio of 0.30. This is due to the densification of the paste microstructure with a reduced porosity. Conversely, the lowest level of true electrical resistivity was obtained for the concretes with the W/B ratio of 0.50. This is because the higher W/B ratio increases the porosity and thus enhances the ionic movement resulting in a reduced electrical resistivity.

The presence of RHA significantly increased the true electrical resistivity of concretes, as evident from Figs. 9 and 10. This is due to the reduced porosity and pore refinement produced by RHA. The electrical resistivity usually increases with lower porosity and smaller pore size [40,41], as the flow of ions through the pore spaces is hindered. In addition, the use of RHA reduces the amount of hydroxyl and alkali ions, which are the main ions that carry charge [42]. Therefore, the electrical resistivity greatly increased in the presence of RHA. Also, the RHA resulted in substantially a high resistivity at 56 days, as obvious from Fig. 9. At this age, the improvement in true electrical resistivity was relatively very high as compared with other properties such as compressive strength. This is probably due to the combined effects of porosity reduction and pozzolanic reaction. A pozzolanic material generally provides a high resistivity despite its low contribution to the compressive strength of concrete [43,44].

The true electrical resistivity of concrete increased in the presence of entrained air-voids. It can be seen from Fig. 9 that the concrete 'C50R0A6' with 5.2% total air content provided a slightly greater resistivity than the concrete 'C50R0A2' containing 1.8% entrapped air content. This is related to the total porosity of these two concretes. The concrete 'C50R0A6' provided a lower total porosity than the concrete 'C50R0A2' because the capillary porosity decreases in the presence of unconnected entrained air-voids [35]. Consequently, the ionic movement was reduced and the concrete resistivity became higher.

3.7. Optimum RHA content

The hardened properties of the concretes were improved gradually with the increased RHA content. All RHA concretes fulfilled

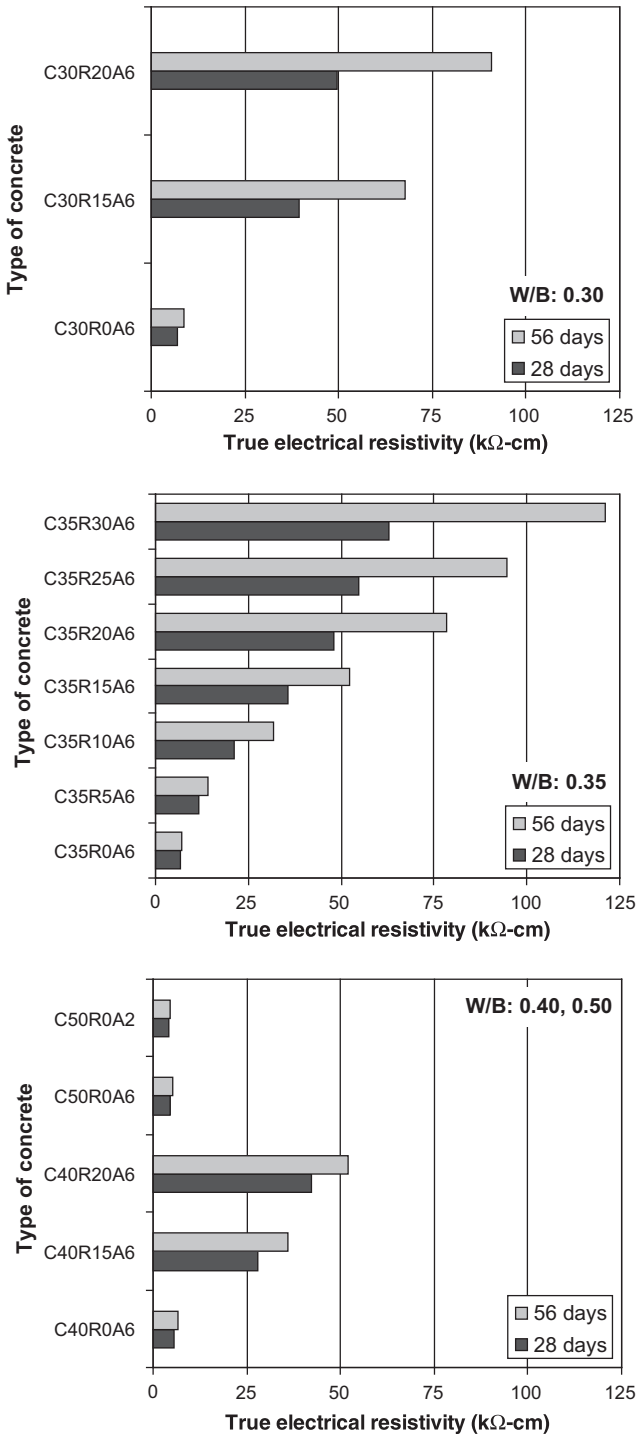

Fig. 9. True electrical resistivity of various concretes.

the performance criteria for the hardened properties tested in the present study. However, the concretes with 15% and 20% RHA provided relatively excellent hardened properties. At the ages of 28 and 56 days, the improvement in the concrete properties, except for true electrical resistivity was less than 6% for each 5% increase beyond 20% RHA content. The true electrical resistivity increased by 14% to 28% for each 5% increase up to 15% RHA content. In contrast, the increase in electrical resistivity became almost double (25–52%) when the RHA content was increased from 15% to 20%. Hence, 15–20% RHA can be considered as the optimum content based on the improvements in the hardened

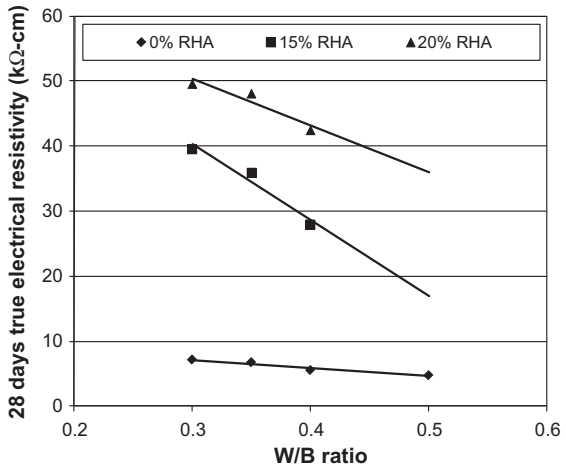

Fig. 10. Effects of W/B ratio and RHA content on the true electrical resistivity of concrete.

properties. However, the RHA content greater than 15% caused to decrease the filling ability of fresh concrete significantly by increasing the surface area of binder. Therefore, the RHA contents greater than 15% needed relatively high dosages of HRWR to achieve the required filling ability. In case of 20–30% RHA, the HRWR dosages required were much higher than the maximum dosage recommended by the manufacture. A high dosage of HRWR may cause the cement setting problem and thus could delay the hydration process in concrete. The demand for the AEA dosages for a given air content was also relatively high for 20% and greater RHA contents. In addition, the mixing and handling difficulties were experienced for the concretes including a RHA content greater than 15% due to excessive cohesiveness or stickiness. Therefore, 15% RHA can be recommended as the optimum RHA content for SCHPC in the context of the present study.

The optimum RHA content also depends on the particle characteristics of rice husk ash. The particle characteristics of RHA can differ based on the production process. It has been reported that the chemically treated RHA possesses greater specific surface area and silica content than conventional RHA [19]. Consequently, the chemically treated RHA shows a higher pozzolanic activity, and thus improves the hardened properties more significantly than conventional RHA [19]. Hence, a lower content of chemically treated RHA will be required to achieve the same level of hardened properties as given by the conventional RHA. However, the requirements for HRWR and AEA dosages will be increased greatly due to the increased surface area of RHA. In addition, the likelihood for the mixing and handling difficulties will be increased for the RHA with a greater specific surface area. Therefore, the optimum content would be lower in case of chemically treated RHA.

4. Conclusions

Based on the experimental results for various SCHPCs produced in the present study, the following conclusions can be drawn:

a. The required filling ability (slump flow) and air content were achieved for all concretes. However, the demands for HRWR and AEA dosages were increased with lower W/B ratio and higher RHA content due to the increased surface area of binder.
b. The hardened properties of the concretes were enhanced with lower W/B ratio due to the improved paste densification resulting from a greater amount of hydration products in the presence of higher binder content.
c. The hardened properties of the concretes were progressively improved with the increased content of RHA because of its microfilling and pozzolanic effects, which improve the microstructure and pore structure of concrete in bulk paste matrix and transition zone.
d. The total porosity of the concretes decreased with lower W/B ratio and higher RHA content. The reduction in total porosity increased the compressive strength, ultrasonic pulse velocity and electrical resistivity, and decreased the water absorption of concrete.
e. The excellent hardened properties were achieved at 15% RHA, which was also suitable to provide the required slump flow and air content with relatively low dosages of HRWR and AEA, respectively. In addition, no mixing and handling difficulties were experienced for the SCHPCs including the RHA content of 15%. Hence, 15% RHA was the optimum RHA content for SCHPC.
f. The increased air content decreased the compressive strength since the air-voids increased the total void content, which reduced the load carrying capacity of concrete. Also, the increase in air content decreased the ultrasonic pulse velocity of concrete, as the increased amount of air-voids delayed the propagation of ultrasonic pulse.
g. The higher air content decreased the total porosity of concrete due to reduced water content and non-connectivity of the entrained air-voids, and thus provided a lower water absorption and a higher electrical resistivity of concrete.

Acknowledgements

The authors are grateful to BASF Construction Chemicals Canada Ltd. for supplying chemical admixtures and to Lafarge North America Inc. for the supply of cement. The cooperation of Renewable Energy Generation Inc. in collecting the RHA required for the research program is also greatly appreciated.

References

[1] Khayat KH. Workability, testing, and performance of self-consolidating concrete. ACI Mater J 1999;96(3):346–53.
[2] Russell HG. ACI defines high-performance concrete. Concr Int 1999;21(2):56–7.
[3] SCCEPG. The European guidelines for self-compacting concrete: specification, production and use. West Midlands, UK: Self-Compacting Concrete European Project Group (SCCEPG), The European Federation of Concrete Admixtures Associations; 2005.
[4] EFNARC. Specifications and guidelines for self-consolidating concrete. Surrey, UK: European Federation of Suppliers of Specialist Construction Chemicals (EFNARC); 2002.
[5] Grünewald S, Walraven JC, Emborg M, Cärlsward J, Hedin C. Test methods for filling ability of SCC. Summary report of workpackage 3.1. Netherlands: Delft University of Technology and Betongindustri; 2004.
[6] Brameshuber W, Uebachs S. Practical experience with the application of self-compacting concrete in Germany. In: Proceedings of the second international symposium on self-compacting concrete. Tokyo, Japan: COMS Engineering Corporation; 2001. p. 687–95.
[7] Bui VK, Montgomery D, Hinczak I, Turner K. Rapid testing method for segregation resistance of self-compacting concrete. Cem Concr Res 2002;32(9):1489–96.
[8] Perez N, Romero H, Hermida G, Cuellar G. Self-compacting concrete, on the search and finding of an optimized design. In: Proceedings of the first North American conference on the design and use of self-consolidating concrete. Illinois, USA: Hanley-Wood, LLC; 2002. p. 101–7.
[9] Khayat KH. Optimization and performance of air-entrained, self-consolidating concrete. ACI Mater J 2000;97(5):526–35.
[10] Kosmatka SH, Kerkhoff B, Panareśe WC, MacLeod NF, McGrath RJ. Design and control of concrete mixtures, 7th ed. Ottawa, Ontario, Canada: Cement Association of Canada; 2002.
[11] Shetty MS. Concrete technology: theory and practice. New Delhi, India: S. Chand and Company Ltd.; 2001.
[12] Hearn N, Hooton RD, Mills RH. Pore structure and permeability. Significance of tests and properties of concrete and concrete-making materials (ASTM STP

169C). Philadelphia, USA: American Society for Testing and Materials. p. 240–62.
[13] Vanwalleghem H, Blontrock H, Taerwe L. Spalling tests on self-compacting concrete. In: Proceedings of the third international symposium on self-compacting concrete. Bagneux, France: RILEM Publications; 2003. p. 855–62.
[14] Hearn N. On the corrosion of steel reinforcement in concrete. In: Proceedings of the 1st structural specialty conference. Montréal, Quebec: Canadian Society for Civil Engineering; 1996. p. 763–74.
[15] Persson B. A comparison between mechanical properties of self-compacting concrete and the corresponding properties of normal concrete. Cem Concr Res 2001;31(2):193–8.
[16] Bouzoubaâ N, Lachemi M. Self-compacting concrete incorporating high volumes of Class F fly ash: preliminary results. Cem Concr Res 2001;31(3):413–20.
[17] Okamura H, Ozawa K. Self-compactable high-performance concrete in Japan. In: Proceedings of the international workshop on high-performance concrete (ACI SP-159). Farmington Hills, Michigan, USA: American Concrete Institute; 1994. p. 31–44.
[18] Mehta PK, Monteiro PJM. Concrete: microstructure, properties, and materials. 3rd ed. New York, USA: McGraw-Hill Companies, Inc.; 2005.
[19] Salas A, Delvasto S, de Gutierrez RM, Lange D. Comparison of two processes for treating rice husk ash for use in high performance concrete. Cem Concr Res 2009;39(9):773–8.
[20] Mahmud HB, Majuar E, Zain MFM, Hamid NBAA. Mechanical properties and durability of high strength concrete containing rice husk ash. In: Proceedings of the eighth CANMET/ACI international conference on fly ash, silica fume, slag and natural pozzolans in concrete (ACI SP-221). Farmington Hills, Michigan, USA: American Concrete Institute; 2004. p. 751–65.
[21] Zhang MH, Malhotra VM. High-performance concrete incorporating rice husk ash as a supplementary cementing material. ACI Mater J 1996;93(6):629–36.
[22] Maeda N, Wada I, Kawakami M, Ueda T, Pushpalal GKD. Chloride diffusivity of concrete incorporating rice husk ash. In: Proceedings of the fifth CANMET/ACI International conferences on recent advances in concrete technology (ACI SP-200). Farmington Hills, Michigan, USA: American Concrete Institute; 2001. p. 291–308.
[23] Zhu W, Bartos PJM. Permeation properties of self-compacting concrete. Cem Concr Res 2003;33(6):921–6.
[24] Vegas P. Rice production and marketing. California, USA: Sage V Foods, LLC, Los Angeles; 2008.
[25] Mehta PK. Rice husk ash – a unique supplementary cementing material. In: Proceedings of the CANMET/ACI international symposium on advances in concrete technology. Ottawa, Canada: Canada Communication Group – Publishing; 1992. p. 407–30.
[26] Safiuddin Md, West JS, Soudki KA. Flowing ability of the binder pastes formulated from self-compacting concretes incorporating rice husk ash. Kuwait J Sci Eng 2010;37(2).
[27] Safiuddin Md, West JS, Soudki KA. A simple technique to estimate the air-entraining admixture dosage for self-consolidating concrete. In: Proceedings of the 10th international conference on concrete engineering and technology. Shah Alam, Selangor Darul Ehsan, Malaysia: University Technology MARA Malaysia; 2009.
[28] Safiuddin Md. Development of self-consolidating high performance concrete incorporating rice husk ash. Ph.D. Thesis. Waterloo, Ontario, Canada: University of Waterloo; 2008.
[29] Safiuddin Md, West JS, Soudki KA. Flowing ability of self-consolidating concrete and its paste and mortar components incorporating rice husk ash. Can J Civ Eng 2010;37(3):401–12.
[30] FM 5-578. Florida method of test for concrete resistivity as an electrical indicator of its permeability. Florida, USA: The Florida Department of Transportation; 2004.
[31] Morris W, Moreno EI, Sagüés AA. Practical evaluation of resistivity of concrete in test cylinders using a Wenner array probe. Cem Concr Res 1996;26(12):1779–87.
[32] Safiuddin Md, Hearn N. Comparison of ASTM saturation techniques for measuring the permeable porosity of concrete. Cem Concr Res 2005;35(5):1008–13.
[33] ACI 201.2R-08. Guide to durable concrete. ACI manual of concrete practice (part 1). Farmington Hills, Michigan, USA: American Concrete Institute; 2008.
[34] Khayat KH, Assaad J. Air void stability in self-consolidating concrete. ACI Mater J 2002;99(4):408–16.
[35] Neville AM. Properties of concrete, 4th ed. New York, USA: John Wiley & Sons, Inc.; 1996.
[36] Zhang MH, Lastra R, Malhotra VM. Rice-husk ash paste and concrete: some aspects of hydration and the microstructure of the interfacial zone between the aggregate and paste. Cem Concr Res 1996;26(6):963–77.
[37] De Sensale GR. Strength development of concrete with rice husk ash. Cement Concr Compos 2006;28(2):158–60.
[38] Yu Q, Sawayama K, Sugita S, Shoya M, Isojima Y. The reaction between rice husk ash and $Ca(OH)_2$ solution and the nature of its product. Cem Concr Res 1999;29(1):37–43.
[39] Naik TR, Malhotra VM. The ultrasonic pulse velocity method. CRC handbook on nondestructive testing of concrete. Florida, USA: CRC Press; 1991.
[40] Hossain KMA. Correlations between porosity, chloride diffusivity and electrical resistivity in volcanic pumice-based blended cement pastes. Adv Cem Res 2005;17(1):29–37.
[41] Tumidajski PJ. Relationship between resistivity, diffusivity and microstructural descriptors for mortars with silica fume. Cem Concr Res 2005;35(7):1262–8.
[42] Claisse P. Transport properties of concrete. Concr Int 2005;27(1):43–8.
[43] Ampadu KO, Torii K. Chloride ingress and steel corrosion in cement mortars incorporating low-quality fly ashes. Cem Concr Res 2002;32(6):893–901.
[44] Roper H. Mineral admixtures in cements for general use and special purposes. In: Proceedings of an engineering foundation conference on advances in cement and concrete. New York, USA: American Society of Civil Engineers; 1994. p. 237–42.